



Neuroradiology Review Article

## Pearls and Pitfalls in the Magnetic Resonance Diagnosis of Dural Sinus Thrombosis: A Comprehensive Guide for the Trainee Radiologist

Vivek Pai<sup>1</sup>, Iram Khan<sup>1</sup>, Yih Yian Sitoh<sup>1</sup>, Bela Purohit<sup>1</sup>

<sup>1</sup>Department of Neuroradiology, National Neuroscience Institute, Singapore.



**\*Corresponding author:**

Bela Purohit,  
Department of Neuroradiology,  
National Neuroscience  
Institute, Singapore.

[purohitbela@yahoo.co.in](mailto:purohitbela@yahoo.co.in)

Received : 13 October 2020

Accepted : 09 November 2020

Published : 28 November 2020

**DOI:**

10.25259/JCIS\_187\_2020

**Quick Response Code:**



### ABSTRACT

Dural sinus thrombosis (DST) is a potentially fatal neurological condition that can be reversed with early diagnosis and prompt treatment. Non-enhanced CT scan is often the first imaging investigation in patients presenting with acute neurological symptoms; however, its poor sensitivity in detecting DST is a major drawback. Magnetic resonance (MR) imaging offers multiple advantages such as excellent contrast resolution and unenhanced venography possibilities, making it the mainstay in the non-invasive diagnosis of DST. However, physiological variations, evolution of thrombi, and incorrect selection/application of MR techniques can lead to false positive and false negative interpretations impacting patient management and outcome. This article discusses the MR techniques useful to diagnose DST and describes pitfalls, with troubleshooting methods, to ensure an accurate diagnosis. We have used multiple diagrammatic illustrations and MR images to highlight pertinent take-home points and to serve as an easy guide for day-to-day clinical practice.

**Keywords:** Dural sinus thrombosis, Magnetic resonance venography, Time-of-flight Magnetic resonance venography, Phase-contrast magnetic resonance venography, Contrast-enhanced magnetic resonance venography

### INTRODUCTION

Dural sinus thrombosis (DST) is a neurological emergency, accounting for 1–2% of all young adult strokes.<sup>[1]</sup> Its clinical presentation varies with location and subsequent evolution of the thrombus. Common presenting complaints include headache, motor deficits, and convulsions. These symptoms are non-specific and overlap with various other neurological diseases, making the clinical diagnosis of DST challenging and often delaying confirmatory investigations.<sup>[2,3]</sup> With prompt treatment, DST can be reversed, but if untreated, it may rapidly progress to brain parenchymal infarction, parenchymal hemorrhages, altered mentation, coma, and death.<sup>[1]</sup>

Radiology is the investigation of choice for the detection of DST. Non-enhanced CT (NECT) is often the initial investigation, mainly due to its widespread availability and quick scan time.<sup>[4]</sup> The classic hyperdense appearance of DST on NECT is seen only in a third of all patients, making the sensitivity of NECT poor.<sup>[5,6]</sup> CT Venogram is often used as a complimentary tool to NECT with a reported sensitivity of 95% in detecting DST. It requires iodinated contrast media to

This is an open-access article distributed under the terms of the Creative Commons Attribution-Non Commercial-Share Alike 4.0 License, which allows others to remix, tweak, and build upon the work non-commercially, as long as the author is credited and the new creations are licensed under the identical terms.

©2020 Published by Scientific Scholar on behalf of Journal of Clinical Imaging Science

delineate a non-enhancing thrombus within the opacified venous system.<sup>[1,4]</sup> CT contrast media pose an increased risk of allergic reactions and nephrotoxicity.<sup>[7]</sup> Furthermore, CT in view of its ionizing radiation is best avoided in pregnancy, an important group of patients vulnerable to DST.<sup>[8]</sup>

Over the years, Magnetic Resonance Imaging (MRI) has been used more frequently for the diagnosis of DST and its complications.<sup>[9,10]</sup> MRI offers multiple advantages which include its non-ionizing property and excellent contrast resolution that help to identify and age DST accurately. Patel *et al.* reported a sensitivity and specificity of 79.2% and 89.9%, respectively, of routine MRI sequences such as spin- and gradient-echo, diffusion-weighted imaging, and inversion recovery in the diagnosis of DST.<sup>[11]</sup> In addition to these MR sequences, multiple MR venography (MRV) techniques are routinely used to evaluate and quantify flow within the dural sinuses. MR venograms can be performed with or without gadolinium administration. MRV has an overall sensitivity and negative predictive value of 93.54% and 90.9%, respectively.<sup>[12]</sup>

Albeit its advantages over CT, MRI suffers a few limitations. Physiological changes in blood flow, temporal evolution of DST, and incorrect selection/application of MR techniques are common sources of erroneous assumption of sinovenous occlusion or patency. These can lead to an inaccurate diagnosis or a missed pathology.

This educational review provides a simplified understanding of the basic principles of commonly used MRI techniques in the diagnosis of DST. We have highlighted common pitfalls encountered with the use of these techniques along with troubleshooting methods, using case-based imaging examples.

## BASIC PRINCIPLES IN THE MR EVALUATION OF DURAL SINUSES

### Spin echo imaging (SEI)

Conventional SEI utilizes two pulses for signal generation; first, a 90° radiofrequency (RF) pulse to tip the magnetization vector, followed by a 180° rephasing pulse. Mobile spins fail to experience the rephasing pulse and hence do not exhibit a signal. Therefore, patent dural sinuses demonstrate “flow voids” or profound hypointensity [Figure 1].<sup>[13,14]</sup>

Bland DST primarily comprises red blood cells. As a result, it evolves similar to a parenchymal hematoma. Replacement of a signal void (“loss of flow void”) within a dural sinus on SEI must raise suspicion of DST and prompt further evaluation of the dural sinus.<sup>[15]</sup>

### Time-of-flight (TOF) MRV

TOF imaging relies on fundamental principles of “flow-related enhancement.” The sequence is a gradient echo-based sequence that achieves saturation and hence signals suppression of stationary protons by virtue of short interval RF pulses. By selecting an orientation perpendicular to venous flow, bright blood images are obtained on account of freshly entering unsaturated protons imparting a signal [Figure 2].

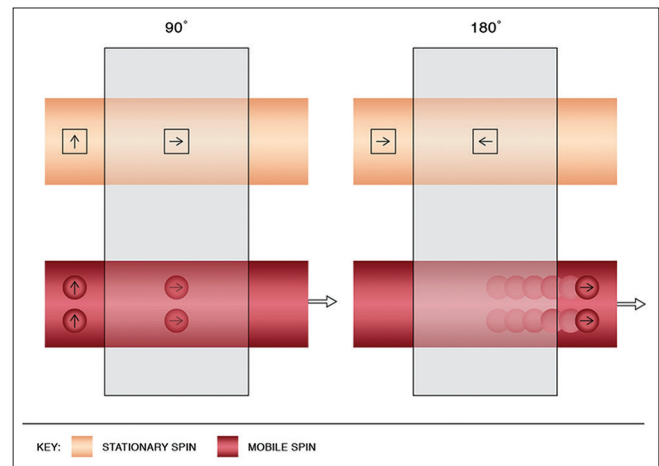


**Figure 1:** Physics of “flow void.” Mobile protons in the dural sinuses exit the imaging slice between the 2 pulses (i.e., do not experience the rephasing 180° pulse) and hence do not generate a signal. Patent dural sinuses, therefore, demonstrate hypointense signals on spin-echo imaging, termed as “flow void.”

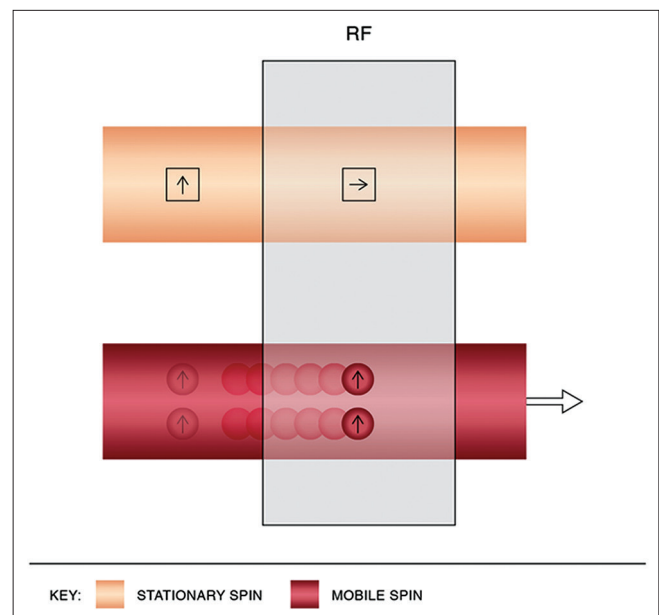


**Figure 2:** Physics of time-of-flight magnetic resonance venography. Using short interval radiofrequency pulses, stationary spins are saturated while mobile spins entering the imaging slice, being unsaturated, impart a bright signal.

Additional saturation bands are applied selectively to nullify signals from adjacent arteries.<sup>[16]</sup>

**Phase-contrast (PC) MRV**

Flowing spins change phase (“phase shift”) as they move along a magnetic gradient. PC techniques use this phenomenon to generate images. It uses additional bipolar gradients to initially induce a phase shift and subsequently to restore it. The net phase difference of stationary protons is zero; however, due to spatial changes, the difference is non-zero for mobile spins [Figure 3].<sup>[16,17]</sup> Voxels in PC imaging therefore represent phase shift data and not signal amplitude, with stationary spins not contributing to the image.<sup>[18]</sup> Using a flow encoding gradient, also known as velocity encoding gradient (VENC), a threshold can be determined to display arterial or venous flow. Higher VENC visualizes arteries and lower VENC visualizes venous flow and cerebrospinal fluid flow (CSF) circulation.<sup>[13,19]</sup>

**Contrast-enhanced (CE) MRV**

Gadolinium chelates are paramagnetic and shorten T1 relaxation time. Following injection, they increase intravascular signal against the background tissues creating a “lumenogram.”<sup>[16]</sup> CE-MRV is typically a 3D-T1 gradient echo-based sequence with short TR and TE to achieve heavily T1W images.<sup>[13,16]</sup> Techniques such as test bolus and bolus tracking are used to ensure that images are obtained in the venous phase. Despite the need for contrast media, CE-MRV provides advantages such as fast data acquisition.<sup>[16]</sup> It also uses thin slices and high matrix which together provide high spatial resolution (independent of flow dynamics) with multiplanar reconstruction capability.<sup>[13,20,21]</sup> CE-MRV has a reported sensitivity and specificity of 83% and 100%, respectively, in the detection of DST.<sup>[22]</sup> A comparison of the different MRV techniques and the MRV parameters used in our department have been summarized in Tables 1 and 2 respectively.

**Table 1:** Comparison of MR venography techniques.<sup>[16,21]</sup>

	TOF-MRV	PC-MRV	CE-MRV
Principle	Flow enhancement	Phase shift	T1 shortening
Sequence	Gradient echo-based	Gradient echo-based	Gradient echo-based
Gadolinium	No	No	Yes
Acquisition time	5–8 min	>15 min*	Approx. 4 min
Background	Partly suppressed	Suppressed	Enhancing lesions seen
Factors for accuracy	Saturation of exogenous signal (arteries)	Operator for selection of appropriate VENC	Scan timing for maximum venous enhancement
Flow velocity	Can detect slow flow	Depends on the VENC	Independent
Flow direction	Not detected	Detected	Not detected
Flow quantification	No	Yes	No

\*Long acquisition time of PC-MRV is due to three gradient directions used to detect flowing spins in all directions. Acquisition time has now been reduced with the help of parallel imaging techniques refer [Table 2].<sup>[16,17]</sup> TOF-MRV: Time-of-flight magnetic resonance venography, PC-MRV: Phase-contrast magnetic resonance venography, CE-MRV: Contrast-enhanced magnetic resonance venography, VENC: Velocity encoding gradient

**Table 2:** MRV parameters used in our department.

	TOF-MRV	PC-MRV	CE-MRV
Acquisition type	2D (axial and coronal)	3D (sagittal left to right)	3D (sagittal left to right)
TR (ms)	23	15	3.4
TE (ms)	4.4	4	1.4
Slice thickness (mm)	2	1.4	2
Slice interval (mm)	2	0.7	1
Flip angle	50	15	25
Matrix	256×192	352×352	356×417
VENC	-	15 cm/s	-
Parallel imaging factor	-	2.5	3
Acquisition time	5 min 25 s	6 min 52 s	2 min 28 s

TOF-MRV: Time-of-flight magnetic resonance venography, PC-MRV: Phase-contrast magnetic resonance venography, CE-MRV: Contrast-enhanced magnetic resonance venography, 2D: Two-dimensional, 3D: Three-dimensional, ms: Millisecond, mm: Millimeter, VENC: Velocity encoding gradient, cm/s: Centimeter per second, min: Minute, s: Second

## POTENTIAL PITFALLS AND ARTIFACTS

A number of false positive and false negative errors are encountered during the MR evaluation of DST. For simplicity, we divide these pitfalls in the following three categories:

### I. Errors on spin-echo sequences

#### Apparent “flow void” in acute DST

An acute thrombus (0–5 days) contains paramagnetic deoxyhemoglobin; hence, it appears isointense on T1W

and hypointense on T2W images. Therefore, an acute thrombus may mimic a flow void seen in patent sinuses on SEI.<sup>[3,23]</sup> In any circumstance, luminal signals must always be evaluated on the gradient recalled echo (GRE) sequence/susceptibility-weighted imaging (SWI) as well. These imaging sequences are very sensitive to field inhomogeneity caused by the paramagnetic acute thrombus, depicted as a hypointense signal (“blooming”/susceptibility artifact). The presence of susceptibility within dural sinuses must raise suspicion of DST and prompt confirmatory venography [Figure 4].<sup>[4,24,25]</sup>

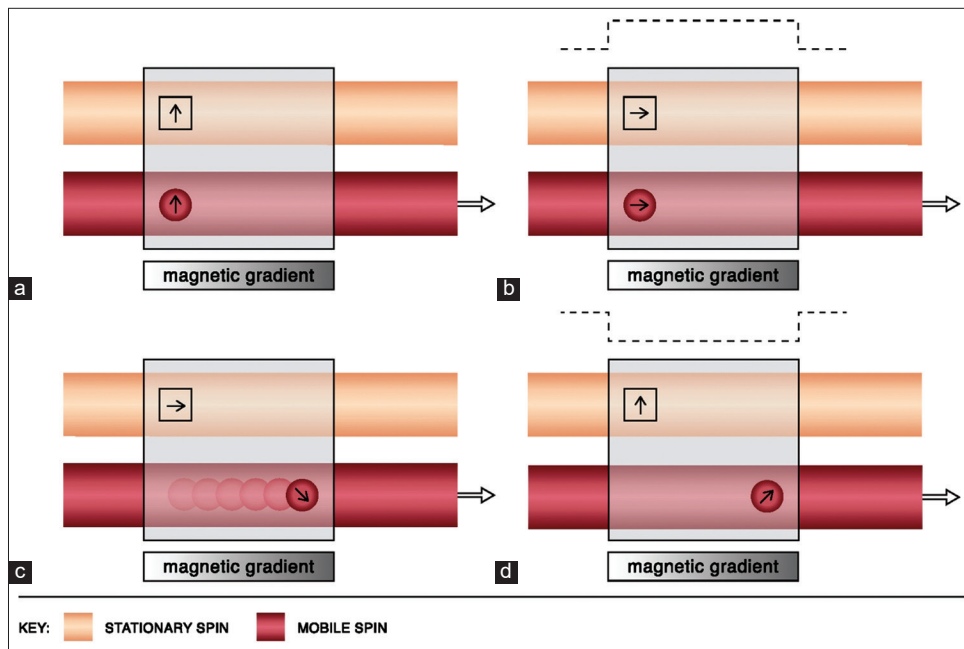


**Figure 3:** Physics of phase-contrast imaging. Line diagram (a) depicts the magnetic vectors of stationary and mobile spins before the use of a bipolar gradient. Line diagram (b) shows the tilting of the magnetic vectors of both stationary and mobile spins by 90° after the application of the first lobe of the bipolar gradient (dotted line). Line diagram (c) shows change in the precession frequency as the mobile protons flow across the magnetic gradient. Line diagram (d) demonstrates the restoration of the stationary vector to its original state upon application of the second lobe of the bipolar gradient. However, a phase difference of the mobile spin persists (i.e., non-zero).

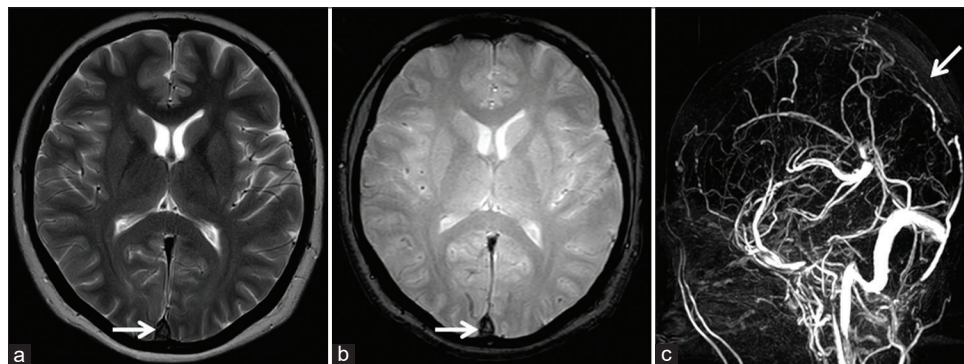


**Figure 4:** Appearance of acute dural sinus thrombosis in a 37-year-old patient presenting with acute headache. Axial T2W image (a) reveals a hypointense signal within the superior sagittal sinus (SSS) mimicking a flow void (arrow). Axial gradient recalled echo image (b) demonstrates “blooming” within the sinus suggesting a thrombus (arrow). Sagittal maximum intensity projection of the phase-contrast magnetic resonance venography (c) confirms an occlusion of the SSS (arrow).

### Loss of flow void: Subacute DST versus slow flow

As the thrombus ages into the subacute phase (6-15 days), deoxyhemoglobin denatures into methemoglobin. This imparts a hyperintense signal on T1W and T2W images, an appearance commonly referred to as “loss of flow void.”<sup>[3]</sup> At this stage, slow flow may mimic DST. With slow transit of venous blood, protons get rephased by the 180° pulse, rendering a bright intraluminal signal. Slow flow typically affects isolated segments and is generally isointense on T1W images.<sup>[3,14]</sup>

It is imperative to make the correct choice of MRV sequence in equivocal cases. TOF-MRV has its limitations in the diagnosis of subacute DST (discussed subsequently). PC-MRV, on the other hand, is insensitive to T1 characteristics of tissue and detects all flowing spins within a given VENC. Hence, optimization of the VENC (lower range) can reliably distinguish slow flow from subacute DST [Figure 5].<sup>[13,18,26]</sup>

In addition, evaluation of luminal signal on the GRE sequence is useful in these circumstances. Methemoglobin, being highly paramagnetic, causes “blooming” on GRE, which would not be expected in slow flow states.<sup>[3,14,24,25]</sup> A subacute thrombus often shows restricted diffusion reflecting its dense microstructure [Figure 6].<sup>[27]</sup>

### Entry slice phenomenon (ESP)

ESP refers to the paradoxical bright intraluminal signal observed on the initial slices of T1W sequences, raising concerns for subacute DST. This occurs due to the flow of unsaturated or “relaxed” spins into an imaging slice on the background of stationary spins saturated by the short TR. The signal intensity fades with successive slices as the blood progressively gets saturated by the rapid RF (short TR) [Figure 7].<sup>[13,14,28]</sup>

ESP is readily identified as it is limited to only the initial imaging slices [Figure 8]. If MRV is considered, PC-MRV is preferable as it allows visualization of flow independent of T1 signals.<sup>[17]</sup> Another easy method to differentiate artifactual flow signal from a true thrombus is repeating acquisition in a different plane. Subacute thrombus shows a bright signal irrespective of orientation of the imaging plane, whereas ESP disappears [Figure 9].<sup>[29]</sup>

## II. Errors on MR venograms

### “Thrombus shine through” effect

The short TR interval used in TOF-MRV makes it a surrogate T1W sequence. Tissues with native intravoxel T1 shortening tend to “shine through,” that is, they appear hyperintense on TOF exams. Thus, methemoglobin in subacute DST

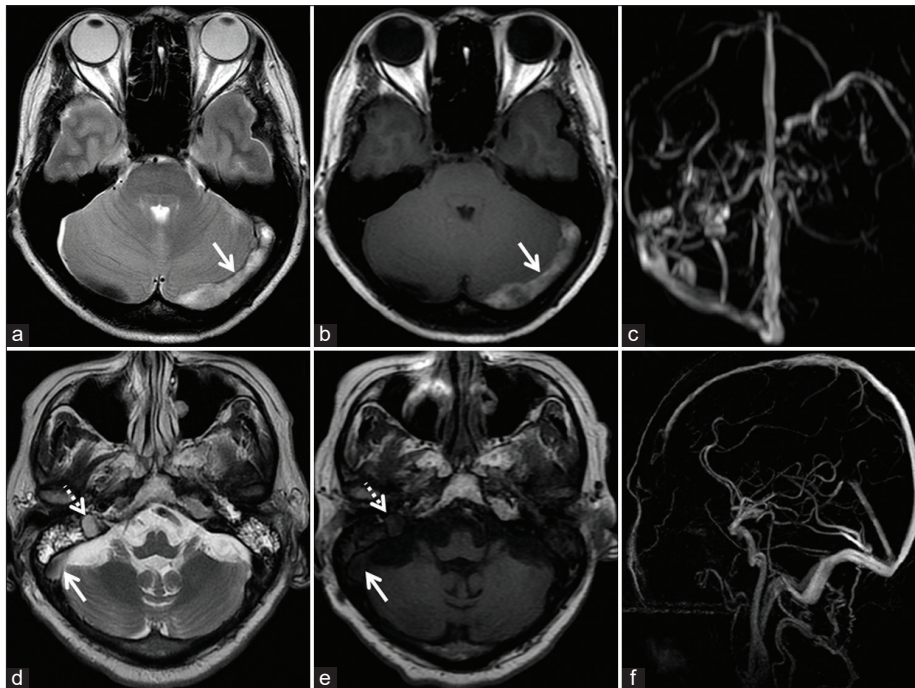


**Figure 5:** Deducing the etiology of loss of flow voids in two different patients. Patient 1 (a-c) was investigated for headache localized to the occipital region. Axial T2W image (a) and axial T1W image (b) show loss of flow void within the left transverse sinus (arrow). Maximum intensity projection (MIP) of the phase-contrast magnetic resonance venography (PC-MRV) (c) confirms the occlusion. Patient 2 (d-f) was imaged for headache associated with blurring of vision. Axial T2W image (d) shows loss of flow void within the right transverse sinus (solid arrow) and sigmoid sinus (dotted arrow). Corresponding axial T1W image (e) shows isointense signal intensity within the sinuses. Sagittal MIP of the PC-MRV (f) confirms patency of the sinuses. The signal alteration is therefore attributed to slow flow.

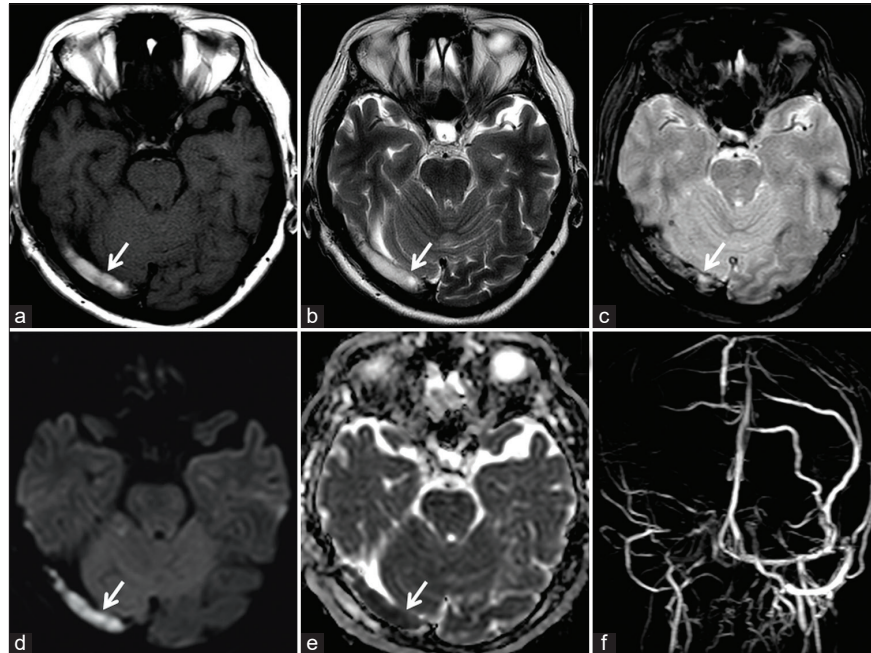


**Figure 6:** Magnetic resonance (MR) appearance of subacute dural sinus thrombosis in a 50-year-old patient. Unenhanced axial T1W image (a) and axial T2W image (b) show hyperintense signal within the right transverse sinus (arrow). Axial gradient recalled echo image (c) shows “blooming” artifact in the right transverse sinus (arrow). Restricted diffusion is also noted on the diffusion-weighted imaging image (d) and apparent diffusion coefficient image (e). Occlusion was confirmed on the phase-contrast MR venography (f).

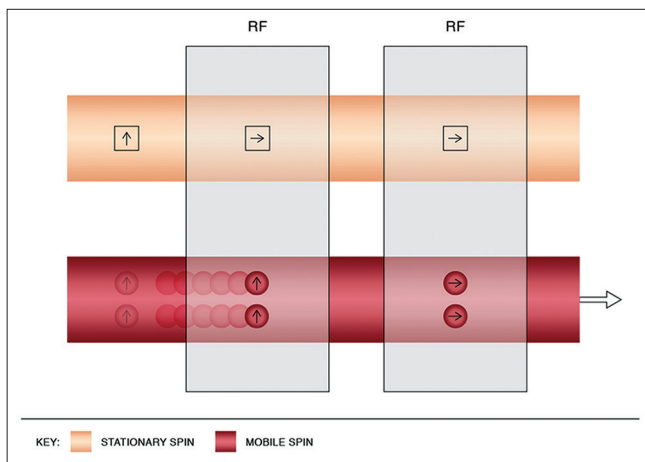


**Figure 7:** Physics of entry slice phenomenon. This results in a bright artifactual signal of mobile spins in the initial images, with gradual fading on the subsequent slices. It occurs due to unsaturated spins flowing into the imaging plane, previously saturated by the short interval radiofrequency pulses. The mobile spins get progressively saturated with resultant hypointense signals as they flow into the imaging volume and experience the repeated pulses.

being T1 hyperintense contributes to an artifactual bright signal on TOF-MRV. Although this is usually not as bright as flow signals, it may still be misinterpreted as patency [Figure 10].<sup>[3,14]</sup> Careful scrutiny of GRE/SWI images (for blooming/susceptibility artifacts) and use of CE-MRV with subtraction help to confirm thrombosis [Figure 11]. PC-

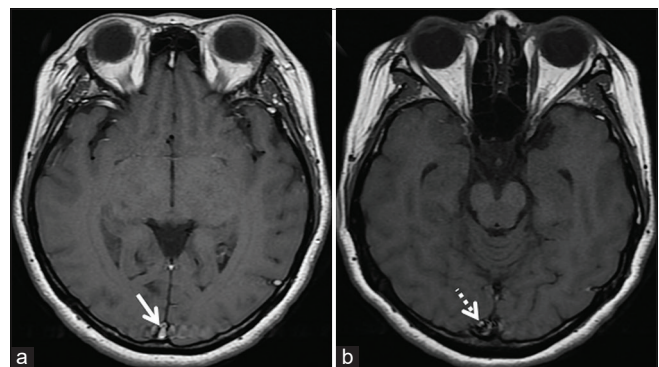


**Figure 8:** Example of entry slice phenomenon. Axial T1W image (a) of an internal acoustic meatus protocol study shows a bright signal in the superior sagittal sinus (arrow) only on the initial slice of the study. The contiguous caudal slice (b) shows fading off, of the signal intensity (dotted arrow).

MRV is very useful in such cases because it is insensitive to T1 shortening effects.<sup>[3,14,17,18]</sup>

#### *In-plane saturation (IPS)*

Flow signals on TOF images are brightest when blood enters perpendicular to the imaging plane. If dural sinuses lie parallel (“in-plane”) to the acquired sections, the spins get saturated and do not contribute signals. This phenomenon of signal loss, in an otherwise patent dural sinus, is known as “in-plane saturation” and must be distinguished from DST.<sup>[30,31]</sup>

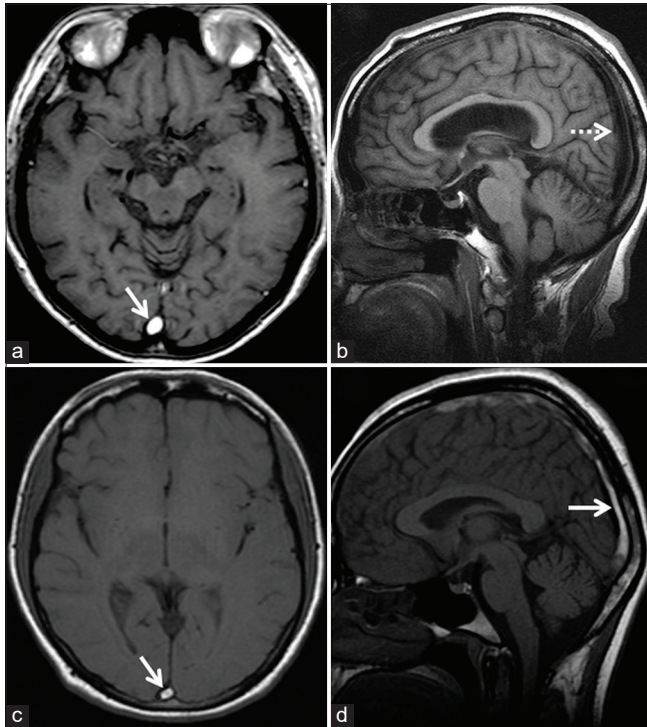


**Figure 9:** Method to differentiate entry slice phenomenon from thrombosis in two different patients. Patient 1 (a and b) was imaged for the investigation of left facial weakness using the internal acoustic meatus protocol. Axial T1W image (a) shows a hyperintense signal in the superior sagittal sinus (SSS) (arrow) only on the initial slice of the imaging volume. Sagittal T1W image (b) of the same patient, obtained during the same examination, demonstrates normal signal void within the SSS. The loss of bright luminal signal on changing orientation of acquisition indicates entry slice phenomenon. Patient 2 (c and d), a 45-year-old patient, was on follow-up for dural sinus thrombosis involving the SSS. Axial T1W image (c) shows a hyperintense signal in the SSS (arrow). The signal intensity persists even after obtaining an orthogonal sagittal T1W image (d). This suggests that the T1 hyperintense signal abnormality (c and d) is a true subacute thrombus rather than an artifact.

Understanding the orientation of acquisition is key to identifying IPS. For example, obtaining coronal TOF venograms aids in the adequate evaluation of the midline sinuses; however, IPS may be troublesome at the torcular and transverse sinuses. For confirmation, orthogonal switching of acquisition may eliminate IPS related signal loss [Figure 12].<sup>[30,31]</sup>

In an attempt to eliminate acquisition of TOF-MRV in two perpendicular planes, a double oblique plane (45° to both coronal and sagittal planes) has been advocated; however, it must be noted that no rectilinear plane can be oriented perpendicular to all dural sinuses in a single acquisition.<sup>[32]</sup> Reconstruction of an obliquely acquired dataset into standard maximum intensity projections also poses challenges due to software limitations.<sup>[32]</sup>

#### ***Hypoplastic dural sinuses and flow gaps on TOF-MRV***

TOF-MRV can detect slow flow, but only up to a minimum limit. Spins flowing slower than this limit encounter the short interval RF pulses and get saturated, resulting in signal loss, also known as “flow gap.”<sup>[32]</sup> This phenomenon is further compounded by coplanar acquisition and is common in hypoplastic dural sinuses. In a study by Ayanzen *et al.*, it was noted that flow gaps were present in 31% of non-dominant transverse sinuses. In fact, they did not observe flow gaps in dominant transverse sinuses or in the rest of the dural venous system, making it imperative to exclude thrombosis before concluding a flow gap.<sup>[32]</sup> The lack of thrombus related signals and use of CE-MRV (independent of the flow dynamics) aid in confirming patency of sinuses [Figure 13].<sup>[32]</sup>

#### ***Signal loss on PC-MRV***

As discussed previously, PC-MRV displays flow information due to phase shifts in mobile protons within a velocity range

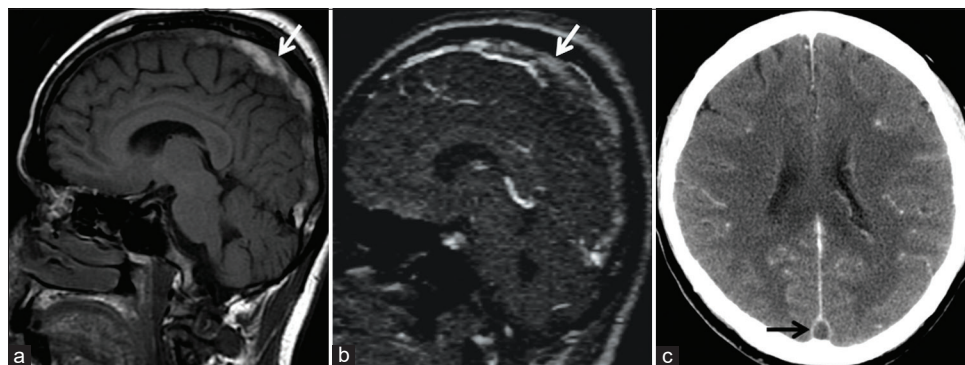


**Figure 10:** Example of “thrombus shine through” in a 58-year-old patient presenting with headache. Unenhanced sagittal T1W image (a) shows a hyperintense subacute thrombus in the superior sagittal sinus (SSS) (arrow). This appears as a faint “shine through” (arrow) on sagittal reconstructions of the time-of-flight MR venography (b) due to the short TR interval used in this imaging technique. Note the filling defect seen in the SSS (arrow) on the follow-up contrast-enhanced CT image (c) confirming sinus occlusion.

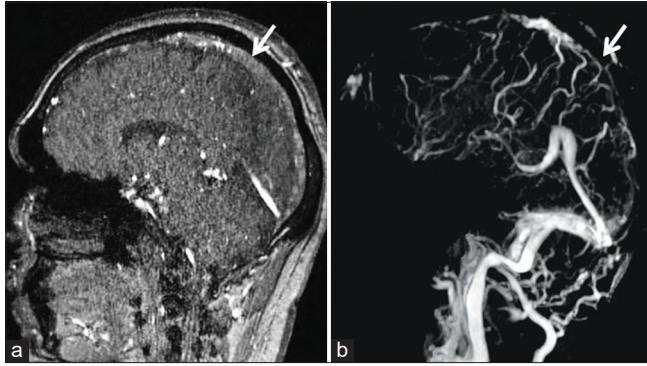


**Figure 11:** Example of “thrombus shine through” due to subacute dural sinus thrombosis (DST) in a 41-year-old patient. Sagittal source time-of-flight magnetic resonance (MR) venography image (a) shows a mild hyperintense signal in the superior sagittal sinus (SSS) (arrow) due to subacute DST. Occlusion of the SSS (arrow) is confirmed on the post-subtraction contrast-enhanced MR venography image (b).

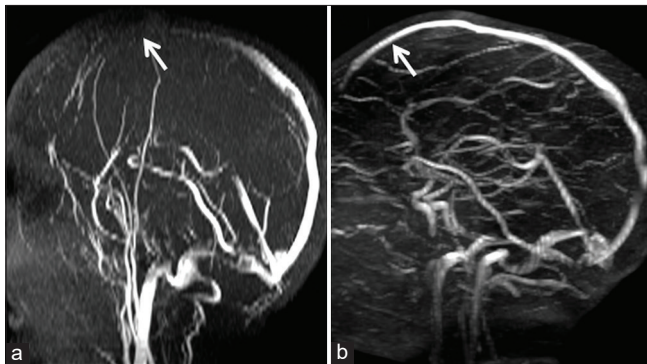


**Figure 12:** Example of in-plane saturation and its correction in a 6-year-old child presenting with febrile convulsions. Maximum intensity projection image of a time-of-flight MR venography (a) acquired in the axial plane demonstrates loss of flow signal in the anterior portion of the superior sagittal sinus (SSS) (arrow). Orthogonal switching to a coronal plane of acquisition (b) helps to confirm patency of the anterior SSS (arrow). The initial signal loss in (a) is hence confirmed to be artifactual due to in-plane saturation.

(VENC) pre-selected by the MR operator. Flow velocity outside the selected VENC may not be displayed, leading to signal loss, mimicking an occlusion. This phenomenon is common in the lateral third of the transverse sinuses due to local flow turbulence caused by arachnoid granulations or stenosis in idiopathic intracranial hypertension (IIH) [Figure 14].<sup>[33]</sup>

Fera *et al.* studied this signal loss in IIH and suggested that lower VENC values (15 cm/s) could not display high-velocity turbulent flow. The signal gap disappeared using a higher VENC (40 cm/s). Careful selection of the VENC is therefore vital in differentiating stenosis from a thrombus.<sup>[26]</sup> CE-MRV being independent of flow/geometry of sinuses and

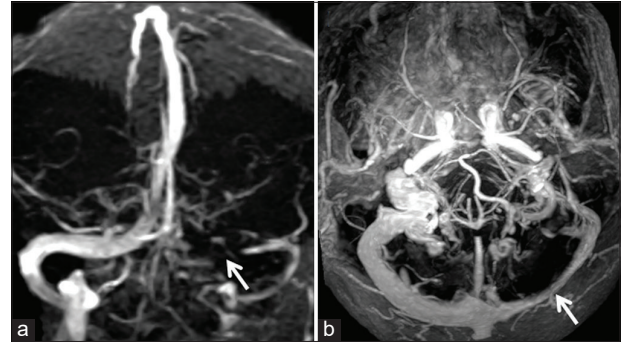


**Figure 13:** Example of “flow gap” in a 70-year-old patient imaged before resection a right frontal meningioma. Time-of-flight magnetic resonance venography (TOF-MRV) image (a) (coronal acquisition) shows signal loss within the proximal left transverse sinus (arrow). Flow signal distally is preserved. Axial maximum intensity projection image of the contrast-enhanced magnetization prepared rapid gradient echo (MPRAGE) (b) confirms hypoplasia of the transverse sinus with adequate luminal enhancement throughout the sinus (arrow). The loss of signal on the TOF-MRV is, therefore, confirmed to be a “flow gap.”



**Figure 14:** Phase-contrast magnetic resonance venography (PC-MRV) (using a velocity encoding gradient [VENC] 15 cm/s) in a 45-year-old female patient with idiopathic intracranial hypertension. Maximum intensity projection of the PC-MRV (VENC 15 cm/s) demonstrates focal symmetric signal losses in lateral portions of both the transverse sinuses due to underlying stenosis (arrows).

along with its high spatial resolution, is an essential adjunct to PC-MRV when the cause of the signal drop remains unclear.<sup>[34]</sup>

### III. Errors on CE MRI

#### Chronic DST

With evolution into chronicity, DST demonstrates T1 isointense and T2 hyperintense signals. Pathologically,

this phase is characterized by intrathrombus fibroblast and capillary proliferation. The end result is the conversion of the thrombus into a fibrotic mass with multiple endothelium-lined channels within. These channels enhance intensely, thereby rendering a false sense of normalcy on contrast-enhanced sequences. Furthermore, chronic DST may lack blooming/susceptibility artifacts (attributed to macrophages clearing denatured hemoglobin from the organizing thrombus), making the sequence unreliable [Figure 15]. Leach *et al.* reported susceptibility artifacts in 90.6% of DST in the initial 7 days as compared to 23.3% in DST older than 8 days.<sup>[35]</sup> Unenhanced MRV is generally adequate to evaluate the lumen in this situation.<sup>[3,35]</sup>

### Non-thrombotic filling defects

Arachnoid granulations are invaginations of arachnoid mater into venous sinuses through dural apertures. They serve as sites for CSF resorption. They can occur anywhere

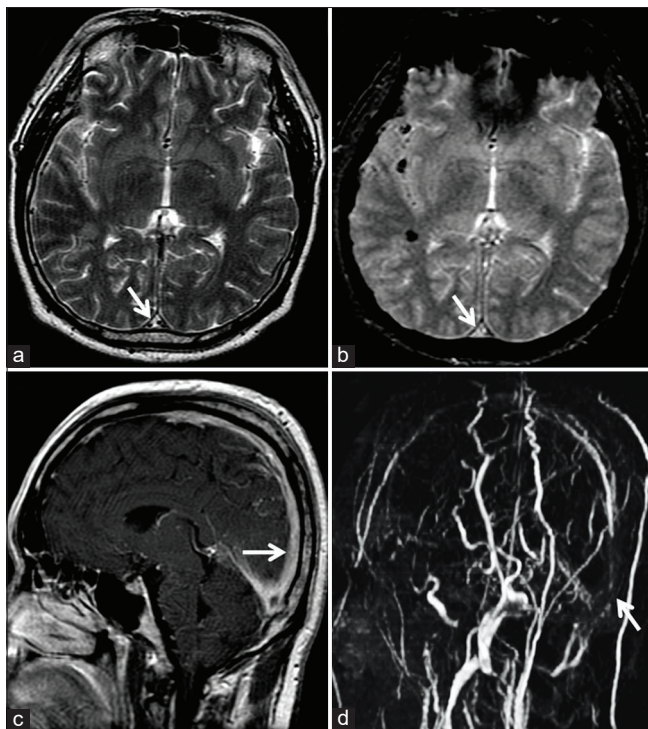


**Figure 15:** Example of chronic thrombosis in a 68-year-old patient on 6 monthly follow-ups after medical management of dural sinus thrombosis involving the superior sagittal sinus (SSS). Axial T2W image (a) shows a hyperintense intraluminal signal within the SSS (arrow) with no blooming on the axial gradient recalled echo image (b). Sagittal post-contrast T1W image (c) shows avid enhancement within the sinus (arrow). Overall, these findings are easy to be misinterpreted as patency. Maximum intensity projection of the phase-contrast MR venography (d) reveals absent flow signals within the SSS (arrow), confirming the diagnosis of a chronic occlusion.

along the dural sinuses, especially along the lateral portion of the transverse sinuses (left predominance) followed by the superior sagittal sinus (SSS).<sup>[3]</sup> On unenhanced T1W images, they appear isointense to hypointense and are always hyperintense on T2W images. Incomplete FLAIR suppression occurs due to altered CSF flow within. Arachnoid granulations vary in size, but when large, may mimic a thrombus [Figure 16].<sup>[3,36]</sup> In addition to their characteristic signal intensity, imaging features which help differentiate these filling defects from thrombosis include their focal, well-defined, round-oval, or lobulated shape and lack of susceptibility artifacts on GRE/SWI sequences.<sup>[36,37]</sup> Arachnoid granulations are never hyperintense on T1W images.<sup>[36]</sup> A frequent, though not consistent finding is the presence of cortical veins entering arachnoid granulations.<sup>[36,37]</sup> Liang *et al.*, in a study of normal structures within dural sinuses, reported the presence of one or more veins in 414 out of 433 (96%) arachnoid granulations.<sup>[36]</sup>

Fibrotic septations are normally found within dural sinuses, often in the straight and transverse sinuses oriented along their long axis. As compared to filling defects in partially recanalized DST, septations produce thin linear filling defects with sharp, well-defined margins. Occasionally, arachnoid granulations may be encountered at the end of septation.<sup>[36]</sup>

Dural sinus stenting has been used for the treatment of IIH with great technical and clinical results. Transverse sinus stenting is known to improve vision, headache, and papilledema in patients with refractory IIH.<sup>[38]</sup> These stents appear as filling defects on CE-MRV; they seldom pose concerns in the presence of an adequate clinical history [Figure 17].

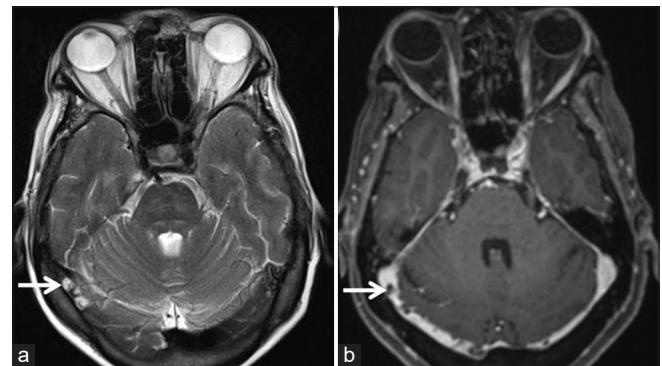


**Figure 16:** Appearance of arachnoid granulations detected incidentally during the magnetic resonance evaluation of a patient with long-standing headache. Axial T2W image (a) shows arachnoid granulations appearing as hyperintense structures (arrows) projecting within the right transverse sinus. Corresponding axial contrast-enhanced T1W image (b) shows them as filling defects within the contrast-enhanced sinus (arrows).

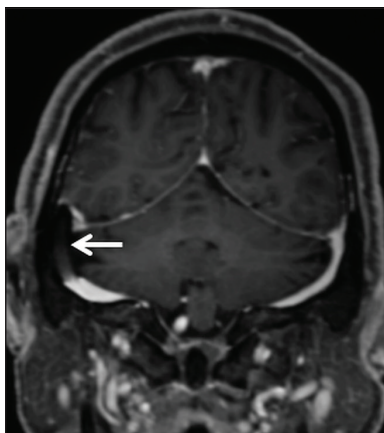


**Figure 17:** Appearance of endovascular stenting of the right transverse sinus, as a part of the management of idiopathic intracranial hypertension. Contrast-enhanced magnetization prepared rapid gradient echo shows a filling defect within the right transverse sinus (arrow) which represents the stent.

## CONCLUSION

MRI as a diagnostic tool has revolutionized the management of DST. DST can be diagnosed using standard MR sequences along with MRV even without contrast administration. A sound understanding of the principles of relevant MR techniques, awareness of imaging appearance of evolving thrombi, as well as potential imaging pitfalls are all crucial for avoiding misdiagnosis. We hope that these image-based diagnostic pearls come in handy, especially for trainee radiologists when dealing with these scans on a routine basis, so as to facilitate optimum management of this clinical scenario.

## Declaration of patient consent

Patient's consent not required as patients identity is not disclosed or compromised.

## Financial support and sponsorship

Nil.

## Conflicts of interest

There are no conflicts of interest.

## REFERENCES

1. Provenzale J, Joseph G, Barboriak D. Dural sinus thrombosis: Findings on CT and MR imaging and diagnostic pitfalls. *Am J Roentgenol* 1998;170:777-83.
2. Canedo-Antelo M, Baleato-González S, Mosqueira A, Casas-Martínez J, Oleaga L, Vilanova JC, *et al.* Radiologic clues to cerebral venous thrombosis. *Radiographics* 2019;39:1611-28.
3. Leach JL, Fortuna R, Jones B, Gaskill-Shipley MF. Imaging of cerebral venous thrombosis: Current techniques, spectrum of findings, and diagnostic pitfalls. *Radiographics* 2006;26:S19-41.
4. Chiewvit P, Piyapittayanan S, Pongvarin N. Cerebral venous thrombosis: Diagnosis dilemma. *Neurol Int* 2011;3:13.
5. Digge P, Prakashini K, Bharath KV. Plain CT vs MR venography in acute cerebral venous sinus thrombosis: Triumphant dark horse. *Indian J Radiol Imaging* 2018;28:280-4.
6. Alsafi A, Lakhani A, Jones LC, Lobotesis K. Cerebral venous sinus thrombosis, a non-enhanced CT diagnosis? *Radiol Res Pract* 2015;2015:1-5.
7. Rodallec M, Krainik A, Feydy A, Hélias A, Colombani JM, Jullès MC, *et al.* Cerebral venous thrombosis and multidetector CT angiography: Tips and tricks. *Radiographics* 2006;26:S5-18.
8. Smith R, Hourihan M. Investigating suspected cerebral venous thrombosis. *Br Med J* 2007;334:794-5.
9. Leach JL, Strub WM, Gaskill-Shipley MF. Cerebral venous thrombus signal intensity and susceptibility effects on gradient recalled-echo MR imaging. *Am J Neuroradiol* 2007;28:940-5.
10. Stam J. Thrombosis of the cerebral veins and sinuses. *N Engl J Med* 2005;352:1791-8.
11. Patel D, Machnowska M, Symons S, Yeung R, Fox AJ, Aviv RI, *et al.* Diagnostic performance of routine brain MRI sequences for dural venous sinus thrombosis. *Am J Neuroradiol* 2016;37:2026-32.
12. Jalli R, Zarei F, Farahangiz S, Khaleghi F, Petramfar P, Borhani-Haghighi A, *et al.* The sensitivity, specificity, and accuracy of contrast-enhanced T1-weighted image, T2\*-weighted image, and magnetic resonance venography in diagnosis of cerebral venous sinus thrombosis. *J Stroke Cerebrovasc Dis* 2016;25:2083-6.
13. Westbrook C, Roth CK, Talbot J. Vascular and cardiac imaging. In: *MRI in Practice*. 4<sup>th</sup> ed. United States: Wiley-Blackwell Publishing Ltd.; 2011. p. 262-89.
14. Pandey S, Hakky M, Kwak E, Jara H, Geyer C, Erbay S. Application of basic principles of physics to head and neck MR angiography: Troubleshooting for artifacts. *Radiographics* 2013;33:113-23.
15. Kumar A, Mukund A, Sharma GL. Dural venous thrombosis-a neglected finding on routine MRI sequences. *Indian J Radiol Imaging* 2006;16:276.
16. Agid R, Shelef I, Scott J, Farb R. Imaging of the intracranial venous system. *Neurologist* 2008;14:12-22.
17. Paoletti M, Germani G, De Icco R, Asteggiano C, Zamboni P, Bastianello S. Intra- and extracranial MR venography: Technical notes, clinical application, and imaging development. *Behav Neurol* 2016;2016:1-9.
18. Wymer D, Patel K, Burke W, Bhatia V. Phase-contrast MRI: Physics, techniques, and clinical applications. *Radiographics* 2020;40:122-40.
19. Ferreira HA, Ramalho J. Basic principles of phase contrast magnetic resonance angiography (PC MRA) and MRV. In: Ramalho JN, Castillo M, editors. *Vascular Imaging of the Central Nervous System: Physical Principles, Clinical Applications, and Emerging Techniques*. 1<sup>st</sup> ed. United States: John Wiley & Sons, Inc.; 2013. p. 137-45.
20. Lövsblad K, Schneider J, Bassetti C, El-Koussy M, Guzman R, Heid O, *et al.* Fast contrast-enhanced MR whole-brain

- venography. *Neuroradiology* 2002;44:681-8.
21. Hu H, Haider C, Campeau N, Huston J, Riederer SJ. Intracranial contrast-enhanced magnetic resonance venography with 6.4-fold sensitivity encoding at 1.5 and 3.0 tesla. *J Magn Reson Imaging* 2008;27:653-8.
  22. Tang Y. Cerebrovenous thrombosis. In: Tang Y, editor. *Atlas of Emergency Neurovascular Imaging*. 1<sup>st</sup> ed. Berlin, Germany: Springer; 2020. p. 57.
  23. Hinman J, Provenzale J. Hypointense thrombus on T2-weighted MR imaging: A potential pitfall in the diagnosis of dural sinus thrombosis. *Eur J Radiol* 2002;41:147-52.
  24. Tang MY, Chen TW, Zhang XM, Huang XH. GRE T2\*-weighted MRI: Principles and clinical applications. *Biomed Res Int* 2014;2014:312142.
  25. Mittal P, Kalia V, Dua S. Pictorial essay: Susceptibility-weighted imaging in cerebral ischemia. *Indian J Radiol Imaging* 2010;20:250-3.
  26. Fera F, Bono F, Messina D, Gallo O, Lanza PL, Auteri W, *et al.* Comparison of different MR venography techniques for detecting transverse sinus stenosis in idiopathic intracranial hypertension. *J Neurol* 2005;252:1021-5.
  27. Favrole P, Guichard J, Crassard I, Bousser M, Chabriat H. Diffusion-weighted imaging of intravascular clots in cerebral venous thrombosis. *Stroke* 2004;35:99-103.
  28. Zand KR, Reinhold C, Haider M, Nakai A, Rohoman L, Maheshwari S. Artifacts and pitfalls in MR imaging of the pelvis. *J Magn Reson Imaging* 2007;26:480-97.
  29. Bianchi D, Maeder P, Bogousslavsky J, Schnyder P, Meuli R. Diagnosis of cerebral venous thrombosis with routine magnetic resonance: An update. *Eur Neurol* 1998;40:179-90.
  30. Lewin JS, Masaryk TJ, Smith AS, Ruggieri PM, Ross JS. Time-of-flight intracranial MR venography: Evaluation of the sequential oblique section technique. *Am J Neuroradiol* 1994;15:1657-64.
  31. Widjaja E, Shroff M, Blaser S, Laughlin S, Raybaud C. 2D time-of-flight MR venography in neonates: Anatomy and pitfalls. *Am J Neuroradiol* 2006;27:1913-8.
  32. Ayanzen RH, Bird CR, Keller PJ, McCully FJ, Theobald MR, Heiserman JE. Cerebral MR venography: Normal anatomy and potential diagnostic pitfalls. *Am J Neuroradiol* 2000;21:74-8.
  33. Higgins J, Gillard JH, Owler BK, Harkness K, Pickard JD. MR venography in idiopathic intracranial hypertension: Unappreciated and misunderstood. *J Neurol Neurosurg Psychiatry* 2004;75:621-5.
  34. Saindane A, Mitchell B, Kang J, Desai N, Dehkharghani S. Performance of Spin-echo and gradient-echo T1-weighted sequences for evaluation of dural venous sinus thrombosis and stenosis. *Am J Roentgenol* 2013;201:162-9.
  35. Leach JL, Wolujewicz M, Strub WM. Partially recanalized chronic dural sinus thrombosis: Findings on MR imaging, time-of-flight MR venography, and contrast-enhanced MR venography. *Am J Neuroradiol* 2007;28:782-9.
  36. Liang L, Korogi Y, Sugahara T, Ikushima I, Shigematsu Y, Takahashi M, *et al.* Normal structures in the intracranial dural sinuses: Delineation with 3D contrast-enhanced magnetization prepared rapid acquisition gradient-echo imaging sequence. *Am J Neuroradiol* 2002;23:1739-46.
  37. Haroun A, Mahafza W, Al Najjar M. Arachnoid granulations in the cerebral dural sinuses as demonstrated by contrast-enhanced 3D magnetic resonance venography. *Surg Radiol Anat* 2007;29:323-8.
  38. Satti SR, Leishangthem L, Chaudry MI. Meta-analysis of CSF diversion procedures and dural venous sinus stenting in the setting of medically refractory idiopathic intracranial hypertension. *Am J Neuroradiol* 2015;36:1899-90.

**How to cite this article:** Pai V, Khan I, Sitoh YY, Purohit B. Pearls and pitfalls in the magnetic resonance diagnosis of dural sinus thrombosis: A comprehensive guide for the trainee radiologist. *J Clin Imaging Sci* 2020;10:77.